

Heterometallic Zn₆Ti₂ Building Block Persistent in Metal-organic Frameworks Based on Asymmetrically Substituted Dicarboxylate Ligands

Hyungphil Chun

Department of Applied Chemistry, College of Science and Technology, Hanyang University, Ansan 426-791, Korea
E-mail: hchun@hanyang.ac.kr

Received January 23, 2014, Accepted February 21, 2014

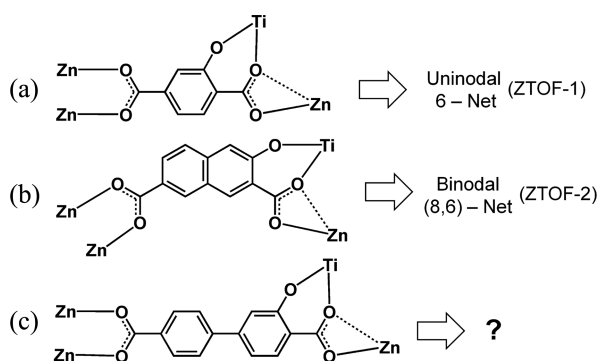
Key Words : Metal-organic framework, Titanium, Heterometallic MOF, Gas sorption

Metal-organic frameworks (MOFs) are coordination-based polymeric networks often noted for their high crystallinity and high level of porosity. Although many MOFs lack the chemical stabilities under ambient conditions, the crystalline porous materials enjoy the status as promising candidates for numerous practical applications thanks to the highly versatile nature of their compositions and structures.¹

The almost infinite variations in the structures of MOFs are governed by two factors, the geometry of secondary building units (SBUs) and organic ligands. A high level of uncertainty is almost always associated with the former, while the latter, in structure-point of view, largely remains invariant during the synthesis of MOFs. Therefore identifying a new SBU with a well-defined geometry is of a paramount importance in the targeted synthesis of new MOFs.² In this context, exploiting two different metals with dissimilar coordination behavior would be highly beneficial because it can significantly deepen the structural chemistry of MOFs.³ It is, however, a challenging task.

We have recently initiated systematic investigations for Zn(II)-Ti(IV) heterometallic MOFs in hopes to benefit from the rich coordination chemistry of Ti(IV) and the inert nature of Ti-O bonds. In order to host the two different metal ions, we used asymmetrically substituted ligands, such as 2-hydroxyterephthalic acid (H₃obdc) (Scheme 1(a)) or 3-hydroxy-2,7-naphthalenedicarboxylic acid (H₃ondc) (Scheme 1(b)), and reported two prototypes of zinc-titanium-organic frameworks (ZTOF-1 and ZTOF-2).⁴

The general applicability of this approach would depend



Scheme 1. Coordination modes of asymmetrically substituted ligands and the nodality of resulting MOFs.

on the possibility of the so-called isorecticular synthesis, and therefore we used an extended version of H₃obdc, 2-hydroxy-4,4'-biphenyldicarboxylic acid (H₃obpdc) in the same synthetic protocols. Our question at the onset of this work was whether it is possible to predict the nodality of heterometallic MOFs obtained from the obpdc³⁻ ligand (Scheme 1(c)). The crystal structure and basic properties of a new MOF thus obtained are reported herein.

A mixture of zinc(II) nitrate, titanium(IV) isopropoxide and H₃(obpdc) reacts under solvothermal conditions in DMF to give a gel-like suspension from which orange-colored rhomboidal crystals grow. We note that the reaction is quite sensitive to the heating rate, and the formation of a competing microcrystalline phase can only be avoided by raising the temperature very slowly (see Experimental section). The X-ray crystal structure was determined using a synchrotron radiation on very small single crystals (< 0.1 mm), and the formula deduced from it is [H₂N(CH₃)₂][Zn₃(μ₃-OH)Ti(obpdc)₃(O₂CH)] (1). The X-ray powder diffraction (XRPD) pattern simulated from the single-crystal structure is dominated by a few strong peaks at low angles in which the experimental patterns show reasonable agreements (Fig. 1).

From mid- to high angles, however, the experimental diffractogram of the as-synthesized samples shows discrepancies from the simulated pattern. This is probably due to the

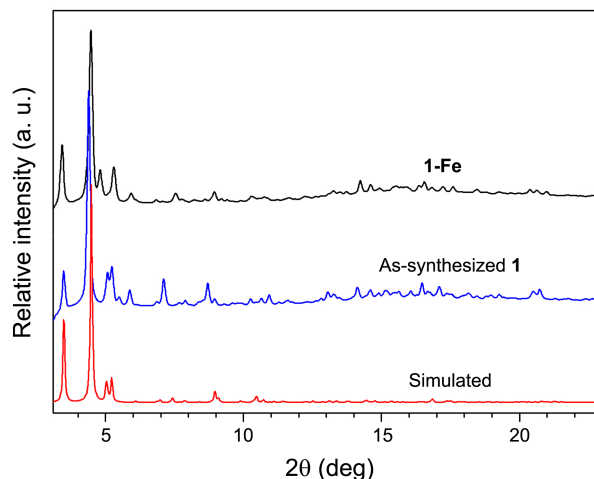


Figure 1. Debye-Scherrer diffraction patterns for 1 and 1-Fe measured using synchrotron X-rays ($\lambda = 1.40000 \text{ \AA}$).

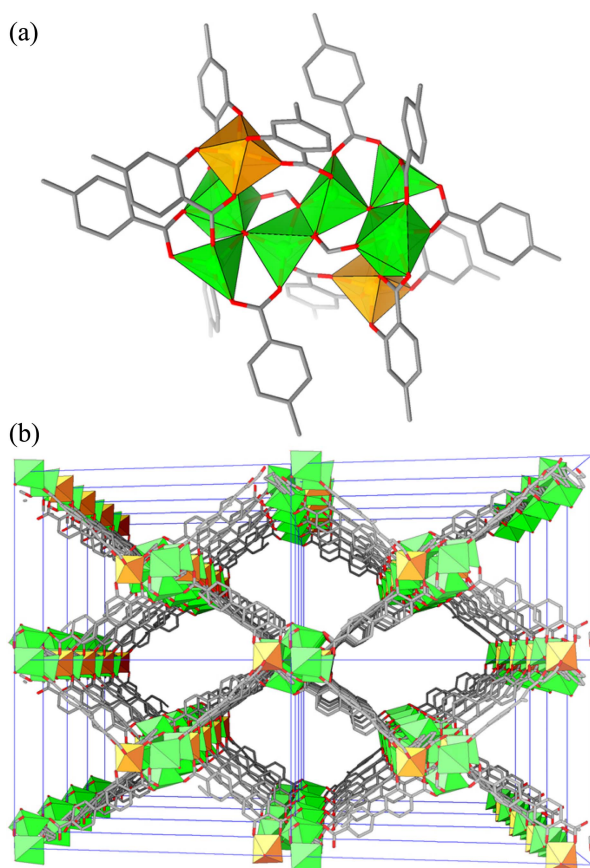


Figure 2. X-ray crystal structure of **1**. (a) Zn₆Ti₂ SBU. (b) Perspective view of the **pcu** net along the *a* axis. Green and orange polyhedra represent Zn and Ti centers, respectively.

flexibility of the biphenyl spacer of the ligand.

The crystal structure of **1** is depicted in Figure 2.

The SBU in **1** is found to be identical to that of ZTOF-1.^{4a} It is composed of two Zn₃Ti units paired with a center of inversion symmetry (Fig. 2(a)). Each unit has the [Zn₃(μ₃-OH)] core capped by a chelated Ti(IV) ion. The bridging formate ligand is believed to be a decomposition product of the solvent (DMF). In the optimized synthesis of **1**, however, a quantitative amount of formic acid was added to the initial reaction mixture in order to improve the yield and crystallinity of the product. Overall the SBU is supported by twelve obpdc ligands which are paired in six sets to propagate along six directions (Fig. 2(b)). Therefore, the entire net of **1** possesses the double-walled primitive cubic net (**pcu**) and is isoreticular to ZTOF-1.

Heterometallic MOFs have not benefited from systematic studies in the past, and therefore the discovery of the Zn₆Ti₂ SBU acting as a 6-connecting node is expected to significantly enrich the structural chemistry of heterometallic MOFs. The successful synthesis of the isoreticular MOF is also interesting because its prototype ZTOF-1 showed considerable stability in ambient air. Therefore, we attempted to measure the stability of **1** under various conditions. To our surprise, however, the evacuated solid of **1** does not maintain the original framework judging from the quick disappear-

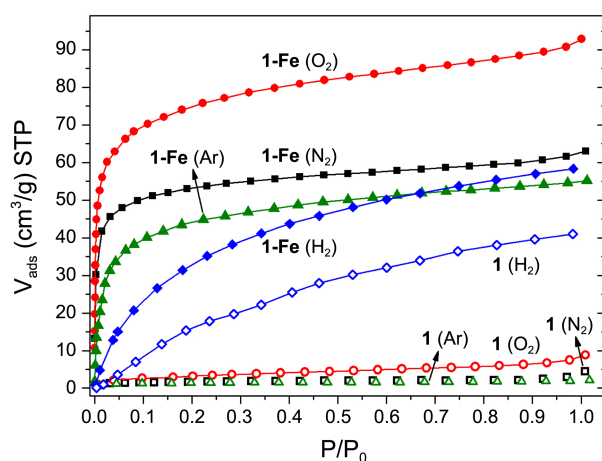


Figure 3. Gas sorption isotherms for **1** and **1-Fe** measured at 77 K. P₀ for H₂ is set to 101 kPa.

ance of the diffraction pattern in XRPD when included solvents are removed. This is against our previous assumption that the rigidity of the SBU and the double-walled structure of ZTOF-1 are responsible for its stability. We believe that the flexible biphenyl linkers do not sustain the evacuated network of **1**. It is noted, however, that the collapsed framework does not completely disintegrate. This is partly supported by the fact that IR spectra do not change after evacuation except for the disappearance of ν(CO) band at 1661 cm⁻¹ from solvent DMF (Fig. S1). In gas sorption studies, the evacuated solid of **1** does not show a significant adsorption of N₂, Ar or O₂ at 77 K (Fig. 3).

Meanwhile, H₂ is adsorbed to a level beyond the surface adsorption at the same temperature and 1 bar (41 cm³/g). The adsorption of H₂ hints at the possibility that **1** may show gated adsorption behavior for other gases under high pressure regions.

The derivation of a permanent porosity by the transmetalation of otherwise unstable MOFs is a highly interesting and important phenomenon.⁵ Thus we attempted similar reactions for **1** to know if the framework can be stabilized in the absence of pore-filling guests. Of many possible choices, we selected Fe³⁺ as the exchanging metal because its oxophilicity should make the trivalent metal compatible to the coordination environment in **1**. The exchange reactions were readily carried out by adding a DMF solution of iron(III) perchlorate DMF solvate in to as-synthesized crystals of **1** soaked in DMF. An immediate color change was observed in the crystals from orange to dark brown. This new material, tentatively labeled as **1-Fe**, shows a powder diffraction pattern similar to **1** (Fig. 1), and ICP-AES analysis reveals that about 16% of total Zn has been replaced by Fe while the content for Ti has not changed at all. These results suggest that Zn²⁺ ions in **1** are selectively substituted by Fe³⁺ while the overall connectivities and the framework structure are retained. In the gas sorption measurements, **1-Fe** clearly shows type I adsorptions for N₂, Ar and O₂ at 77 K, implying considerable stabilization of the void framework **1** (Fig. 3 and Fig. S2). The fact that there is no dramatic improvement

in the uptake of H₂ or that the amounts of N₂, Ar and O₂ adsorbed at P₀ ~ 1 are far below the level expected from the crystal structure of **1**⁶ do not discourage the effort for post-synthetic stabilizations because the working principle is proven and because it leaves much room for improvements, for example, by using other metal ions.

In conclusion, the Zn₆Ti₂ SBU appears to be a persistent and preferably formed building block when asymmetrically substituted, linear dicarboxylate ligands are used. Despite the complexity of the composition and connectivity, the new SBU possesses the nodal geometry of distorted octahedron leading to a simple, 6-connected topology.

Experimental

Materials and Methods. All the reagents were commercially available and used as received except for H₃(obpdc) which was purified by recrystallization before use. IR data were recorded on KBr pellets using a Varian FTS 1000 instrument.

Synthesis of [H₂N(CH₃)₂][Zn₃(μ₃-OH)Ti(obpdc)₃(O₃CH)] (1). Titanium(IV) isopropoxide (29.6 μL, 0.10 mmol) was added to a solution of H₃obpdc (77.7 mg, 0.30 mmol) in DMF (3.5 mL) to form an orange colored turbid mixture. After stirring for 30 min zinc nitrate hexahydrate (51.4 mg, 0.17 mmol) and formic acid (3.8 μL, 0.1 mmol) were added to it. The final mixture was well-stirred for 2 h at room temperature and then filtered. The solution was heated in a sealed glass vial with the following steps: 1 day at 75 °C, 2 days at 95-100 °C and 1 day at 120 °C. The product was separated from the orange-colored suspension, thoroughly washed with fresh DMF and soaked in dichloromethane before drying under vacuum at room temperature for 12 h and then at 100 °C for 5 h (42.7 mg, 68%). Calcd: C, 48.4; H, 2.8; N, 1.3; Ti, 4.3%. Found: C, 48.7; H, 2.9; N, 1.2; Ti, 4.1%.

X-ray Powder Diffraction. X-ray powder diffraction patterns were recorded at the 2D SMC beamline of the Pohang Accelerator Laboratory, Korea. Crystalline samples were thoroughly ground in an agate mortar and packed in a capillary tube (0.3 mm diameter). Debye-Scherrer diffraction data were collected on an ADSC Quantum-210 detector with a fixed wavelength (λ = 1.40000 Å) and an exposure of 60 sec. The ADX program⁷ was used for data collection, and Fit2D program⁸ was used to convert the 2D to 1D patterns.

X-ray Single-crystal Diffraction. Single-crystals of as-synthesized **1** were directly picked up from the mother liquor with a cryoloop attached to a goniocenter, and transferred to a cold stream of liquid nitrogen (-173 °C). The data collection was carried out using synchrotron X-ray on a ADSC Quantum 210 CCD detector with a silicon (111) double-crystal monochromator at 2D SMC beamline of the Pohang Accelerator Laboratory, Korea. The ADSC Quantum-210 ADX program⁷ was used for data collection, and HKL3000sm (Ver. 703r)⁹ was used for cell refinement, data integration, and absorption correction. After space group determination, the structures were solved by direct methods

and subsequent difference Fourier techniques (SHELXLTL).¹⁰ All the non-hydrogen atoms were refined anisotropically, and hydrogen atoms were added to their geometrically ideal positions. The diffused electron densities in the void space could not be modeled properly, and were removed from the reflection data using the SQUEEZE routine of PLATON.¹¹ The results of SQUEEZE process were attached to the CIF file. The crystal data and results of structure refinements are summarized in Table S1. Crystallographic data for the structure reported here have been deposited with CCDC (Deposition No. CCDC-981813 (1)). These data can be obtained free of charge via <http://www.ccdc.cam.ac.uk/conts/retrieving.html> or from CCDC, 12 Union Road, Cambridge CB2 1EZ, UK, E-mail: deposit@ccdc.cam.ac.uk

Gas Sorption. Gas sorption isotherms were measured in a bath of liquid nitrogen (77 K) with a Belsorp Mini-II. The gases used were of the highest quality available (N60 for H₂, N50 for Ar and N₂, and N45 for O₂). Typically, 100-150 mg of solvent-exchanged samples were evacuated under a dynamic vacuum at room temperature for 12 h. The equilibrium criteria were set consistent throughout all the measurements (change in adsorption amounts less than 0.1 cm³/g within 180 sec). Complete gas sorption isotherms are shown in Fig. S2.

Acknowledgments. This research was supported by the Basic Science Research Program through the National Research Foundation of Korea (2012R1A1A2004333). We thank the Pohang Accelerator Laboratory for beam line use (2013-3rd-2D-009).

Supporting Information. Summary of crystal data, FT-IR spectra, complete gas sorption isotherms and crystallographic data in CIF format for **1**.

References

- (a) Furukawa, H.; Cordova, K. E.; O'Keeffe, M.; Yaghi, O. M. *Science* **2013**, *341*, 1230444. (b) Wang, C.; Liu, D.; Lin, W. *J. Am. Chem. Soc.* **2013**, *135*, 13222. (c) Yoon, M.; Suh, K.; Natarajan, S.; Kim, K. *Angew. Chem. Int. Ed.* **2013**, *52*, 2688. (d) Zhang, Z.; Zhao, Y.; Gong, Q.; Li, Z.; Li, J. *Chem. Commun.* **2013**, 653. (e) Dhakshinamoorthy, A.; Alvaro, M.; Garcia, H. *Chem. Commun.* **2012**, *48*, 11275. (f) Bae, Y.-S.; Snurr, R. Q. *Angew. Chem. Int. Ed.* **2011**, *50*, 11586. (g) Allendorf, M. D.; Schwartzberg, A.; Stavila, V.; Talin, A. A. *Chem. Eur. J.* **2011**, *17*, 11372. (h) D'Alessandro, D. M.; Smit, B.; Long, J. R. *Angew. Chem. Int. Ed.* **2010**, *49*, 6058. (i) McKinlay, A. C.; Morris, R. E.; Horcajada, P.; Férey, G.; Gref, R.; Couvreur, P.; Serre, C. *Angew. Chem. Int. Ed.* **2010**, *49*, 6260. (j) Horike, S.; Shimomura, S.; Kitagawa, S. *Nature Chem.* **2009**, *1*, 695. (k) Lee, J. Y.; Farha, O. K.; Roberts, J.; Scheidt, K. A.; Nguyen, S. T.; Hupp, J. T. *Chem. Soc. Rev.* **2009**, *38*, 1450. (l) Czaja, A. U.; Trukhan, N.; Müller, U. *Chem. Soc. Rev.* **2009**, *38*, 1284. (m) Kuppler, R. J.; Timmons, D. J.; Fang, Q.-R.; Li, J.-R.; Makal, T. A.; Young, M. D.; Yuan, D.; Zhao, D.; Zhuang, W.; Zhou, H.-C. *Coord. Chem. Rev.* **2009**, *253*, 3042.
- A comprehensive review on the SBUs found in known MOFs is available: Tranchemontagne, D. J.; Mendoza-Cortés, J. L.; O'Keeffe, M.; Yaghi, O. M. *Chem. Soc. Rev.* **2009**, *38*, 1257.
- (a) For the classification of heterometallic MOFs, see Hong, K.;

- Chun, H. *Chem. Commun.* **2013**, 10953. (b) Das, M. C.; Xiang, S.; Zhang, Z.; Chen, B. *Angew. Chem. Int. Ed.* **2011**, *50*, 10510.
4. (a) Hong, K.; Bak, W.; Chun, H. *Inorg. Chem.* **2013**, *52*, 5645. (b) ref. 3a.
5. (a) Song, X.; Oh, M.; Lah, M. S. *Inorg. Chem.* **2013**, *52*, 10869. (b) Wei, Z.; Lu, W.; Jiang, H.-L.; Zhou, H.-C. *Inorg. Chem.* **2013**, *52*, 1164.
6. According to PLATON,¹¹ the solvent-accessible void in **1** is estimated to be 63% of the total crystal volume.
7. Arvai, A. J.; Nielsen, C. *ADSC Quantum-210 ADX Program*; Area Detector System Corporation; Poway, CA, USA, 1983.
8. Hammersley, A. *Fit2D Program*, ESRF; 6 Rue Jules Horowitz, BP 220 38043, Grenoble CEDEX 9, France.
9. Otwinowski, Z.; Minor, W. *Methods in Enzymology*; Carter, C. W., Jr., Sweet, R. M., Eds.; Academic Press: New York, 1997; Vol. 276, Part A, p 307.
10. Sheldrick, G. M. *SHELXTL-PLUS, Crystal Structure Analysis Package*; Bruker Analytical X-Ray, Madison, WI, USA, 1997.
11. Spek, A. L. *J. Appl. Cryst.* **2003**, *36*, 7.
-